Journal of Solid State Chemistry **158,** 254–259 (2001)
doi:10.1006/jssc.2001.9101, available online at http://www.idealibrary.com on IDEAL®

Raman and Infrared Spectroscopic Study of $Ce_{1-x}M_xVO_{4-0.5x}$ (M=Pb, Sr, and Ca) and $Ce_{1-x}Bi_xVO_4$ Solid Solutions

T. Hirata

National Research Institute for Metals, 1-2-1 Sengen, Tsukuba, Ibaraki 305-0047 Japan
E-mail: hirata@nrim.go.jp

and

A. Watanabe

National Institute for Research in Inorganic Materials, 1-1 Namiki, Tsukuba, Ibaraki 305-0044 Japan
E-mail: watanakt@nirim.go.jp

Received September 26, 2000; in revised form November 19, 2000; accepted December 19, 2000

Raman and infrared spectroscopic studies of $Ce_{1-x}M_xVO_{4-0.5x}$ (M = Pb, Sr, and Ca) and $Ce_{1-x}Bi_xVO_4$ solid solutions have been performed. When aliovalent or isovalent cations with similar/different ionic radii were substituted for Ce in $CeVO_4$ to form the substitutional solid solutions, it was found that the valence and/or ionic radii of the substitutes dominated the solid solubility limit, producing different lattice parameter changes/distinctive spectral features with x in $Ce_{1-x}M_xVO_{4-0.5x}$ and $Ce_{1-x}Bi_xVO_4$. Particularly, the substitution of aliovalent cations, which causes a change in oxygen stoichiometry to preserve the charge neutrality, led to the emergence of several broad bands in the Raman spectra of $Ce_{1-x}M_xVO_{4-0.5x}$ whereas they were absent in $Ce_{1-x}Bi_xVO_4$. The x-dependence of frequency, linewidth, and intensity of the Raman/infrared modes is presented and discussed in order to draw a spectroscopic distinction between $Ce_{1-x}M_xVO_{4-0.5x}$ and $Ce_{1-x}Bi_xVO_4$ solid solutions.

Key Words: **$CeVO_4$; $Ce_{1-x}M_xVO_{4-0.5x}$ (M = Pb, Sr, and Ca); $Ce_{1-x}Bi_xVO_4$; Raman and infrared spectra; aliovalent and isovalent cation substitution; solid solubility limit.**

INTRODUCTION

The tetragonal cerium vanadate $CeVO_4$, which consists of VO_4 tetrahedra and CeO_8 bisdisphenoids (1–3), has space group symmetry D_{4h}^{19}–$I4_1/amd$ ($Z = 4$) with lattice parameters $a = 7.004$ Å and $c = 6.4972$ Å. $CeVO_4$ is regarded as a p-type semiconductor from measurements of electrical conductivity and the Seebeck coefficient (4, 5). Of late, Watanabe (4) has investigated a series of substitutional solid solutions, $Ce_{1-x}M_xVO_{4-0.5x}$ (M = Pb, Sr, and Ca) and $Ce_{1-x}Bi_xVO_4$, with various x values. There was a remarkable enhancement in electrical conductivity in $Ce_{1-x}M_xVO_{4-0.5x}$ over $Ce_{1-x}Bi_xVO_4$ relative to $CeVO_4$, depending on the nature as well as the amount of the substitutes; it is expected that the valence and/or ionic radii of the cations substituted for Ce could dominate the formation of $Ce_{1-x}M_xVO_{4-0.5x}$ and $Ce_{1-x}Bi_xVO_4$ solid solutions.

With respect to the oxidation state of Ce in $CeVO_4$, X-ray absorption spectroscopy has established that the cerium valence in $CeVO_4$ is 3+, whereas the vanadium atom remains in the pentavalent state (5+) (4, 6). Consequently, a change in oxygen stoichiometry amounting to $4 - 0.5x$ is induced to preserve the charge neutrality providing O^{2-}, when aliovalent cations (Pb^{2+}, Sr^{2+}, and Ca^{2+}) are substituted for Ce^{3+} in $CeVO_4$ to form $Ce_{1-x}M_xVO_{4-0.5x}$. It should be noted that oxygen stoichiometry is an influential factor in characterizing the physical/phonon properties of oxides, as well-documented in high T_c oxide superconductors (7–10), which led us toward our interest in the present work.

The present work is concerned with Raman and infrared spectroscopic investigation of $Ce_{1-x}M_xVO_{4-0.5x}$ and $Ce_{1-x}Bi_xVO_4$ solid solutions that will provide valuable information on different lattice distortions when aliovalent or isovalent cations with different/similar ionic radii are substituted for Ce^{3+} (11, 12).

EXPERIMENTAL

Substitutional solid solutions $Ce_{1-x}M_xVO_{4-0.5x}$ (M = Pb, Sr, and Ca) and $Ce_{1-x}Bi_xVO_4$ with various x values were prepared by a solid state reaction technique, details of which are given elsewhere (4). The solid solution process was monitored by DTA (dif-

0022-4596/01 $35.00

TABLE 1

Solid solution	dc/dx (Å/frac.)	da/dx (Å/frac.)	x_{max}
$Ce_{1-x}Pb_xVO_{4-0.5x}$	+0.0190	−0.1540	0.10
$Ce_{1-x}Sr_xVO_{4-0.5x}$	−0.0560	−0.1720	0.21
$Ce_{1-x}Ca_xVO_{4-0.5x}$	−0.2477	−0.4545	0.41
$Ce_{1-x}Bi_xVO_4$	−0.0448	−0.0975	0.68

Note. Lattice parameters of $CeVO_4$: $a = 7.4016(1)$ Å and $c = 6.4980(1)$ Å. Ionic radii of the cations substituted for Ce^{3+} with 1.14 Å: Ca^{2+}, 1.12 Å; Sr^{2+}, 1.26 Å; Pb^{2+}, 1.29 Å; and Bi^{3+}, 1.17 Å.

ferential thermal analysis) combined with TG (thermogravimetry).

The lattice parameters of the reaction products were determined by X-ray powder diffraction with Cu$K\alpha$ radiation. Raman scattering measurements were performed with pellets by a Dilor Raman spectrometer (Super Labram); the scattered light from the samples was collected with a CCD (charge-coupled device) detector, A 514.5-nm line from the Ar^+ laser was used as the radiation source. Incident laser power was limited to 1.0 mW in order to minimize a possibility of sample heating. All Raman spectra were collected in a back-scattering configuration. Infrared spectra were recorded at room temperature by a Fourier transform infrared spectrometer (JEOR 100), with a resolution of 4 cm^{-1} in the wavenumber region of 400 to 4000 cm^{-1}; KBr powder was used as a reference to obtain infrared absorption spectra of pulverzied samples with KBr.

RESULTS AND DISCUSSION

Lattice Contraction

Lattice parameters a and c decreased with x for $Ce_{1-x}M_xVO_{4-0.5x}$ (M = Pb, Sr, and Ca) and $Ce_{1-x}Bi_xVO_4$, with the exception that only the lattice parameter c slightly increased (nonlinearly) with x for $Ce_{1-x}Pb_xVO_{4-0.5x}$ (4). Table 1 lists lattice parameter changes with x, i.e., da/dx and dc/dx, along with x_{max}—the solid solubility limit for each solid solution. We note that the valence and/or ionic radii of the substitutes dominate the values of dc/dx (da/dx) as well as x_{max}. The highest x_{max} and small values of $|dc(a)/dx|$ are apparent for $Ce_{1-x}Bi_xVO_4$. This is possible because Bi^{3+} (1.17 Å) has about the same ionic radius as Ce^{3+} (1.14 Å) (13) besides being isovalent, which facilitates the substitution of Bi for Ce in $CeVO_4$.

However, the substitution of aliovalent Ca^{2+} (1.12 Å), which has almost the same ionic radius as Ce^{3+} (1.14 Å), reduces the x_{max} while confining $|dc(a)/dx|$ to relatively high values. The replacement by the cations, whose ionic radii and valence are different from those of Ce, reduces significantly the x_{max} as well as the values of $|dc(a)/dx|$, as revealed in $Ce_{1-x}Sr_xVO_{4-0.5x}$ and $Ce_{1-x}Pb_xVO_{4-0.5x}$. While the positive value of dc/dx for $Ce_{1-x}Pb_xVO_{4-0.5x}$ is unique and is not well understood, the cell volume of $CeVO_4$ decreases, i.e., lattice contracts on substitution of all the substitutes in the plot of cell volume V as a function of x as shown in Fig. 1. Because of $dV/dx = a[2c(da/dx) + a(dc/dx)]$, effects of the valence and/or ionic radii of the substitutes are also implicated even in the x-dependence of V.

Raman Spectra

Figure 2 shows the Raman spectra of $Ce_{1-x}M_xVO_{4-0.5x}$ (M = Pb, Sr, and Ca) and $Ce_{1-x}Bi_xVO_4$ as a function of x in the range 200–1000 cm^{-1}, along with that of $CeVO_4$ for reference. The present spectrum of $CeVO_4$ is comparable to that found in the literature (14). In the Raman spectrum of $CeVO_4$, five Raman modes are observed at 261, 372, 461, 771, and 847 cm^{-1}. The 372-, 461-, 771-, and 847-cm^{-1} modes are assigned as $A_{1g} + B_{1g}$ deformation (v_2), $E_g + B_{2g}$ deformation (v_4), E_g asymmetric stretch (v_3), and A_{1g} symmetric stretch (v_1), respectively (14–16), while no assignment is made for the 261-cm^{-1} mode.

We notice that the B_{2g} asymmetric stretch mode (v_3) at 784 cm^{-1} accompanies the E_g asymmetric stretch mode (v_3) at 771 cm^{-1}, exhibiting a sign of two resolved peaks.

In addition, a shoulder is apparent on the high-frequency side ($\sim$860 cm^{-1}) of the A_{1g} symmetric stretch mode at 847 cm^{-1}, and there is a small peak observed around 220 cm^{-1}, as detected in the literature (14). The shoulder at approximately 860 cm^{-1} is not due to other vanadate species or any impurity phase, the presence of which is ruled out by X-ray diffraction.

When we compare the Raman spectra of $Ce_{1-x}M_xVO_{4-0.5x}$ (M = Pb, Sr, and Ca) with those of $Ce_{1-x}Bi_xVO_4$, several points are noticeable. On substitution of the aliovalent cations (Ca^{2+}, Pb^{2+}, and Sr^{2+}), broad Raman bands emerge at $\sim$495, 705, and 912 cm^{-1}, which gain intensity with x. Note that the appearance of these

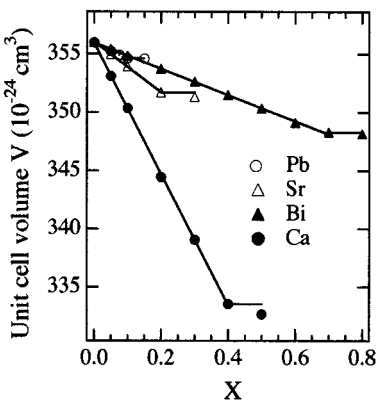

FIG. 1. Unit cell volume change of $Ce_{1-x}M_xVO_{4-0.5x}$ (M = Pb, Sr, and Ca) and $Ce_{1-x}Bi_xVO_4$ with x.

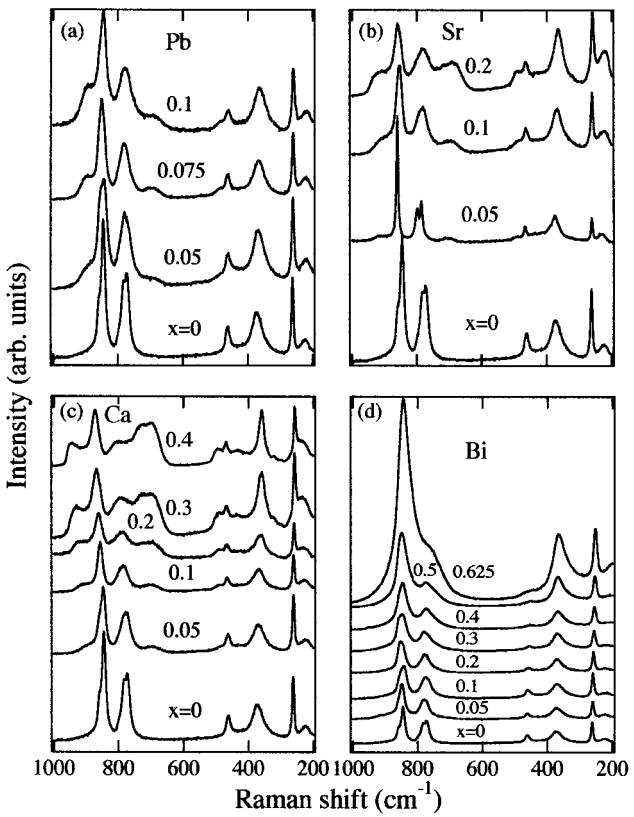

FIG. 2. The Raman spectra of $Ce_{1-x}M_xVO_{4-0.5x}$ (M = Pb, Sr, and Ca) and $Ce_{1-x}Bi_xVO_4$ as a function of x in the range 200–1000 cm^{-1}, along with that of $CeVO_4$ for reference, $x = 0, 0.05, 0.075$, and 0.1 (from bottom to top) for $Ce_{1-x}Pb_xVO_{4-0.5x}$ (a); $x = 0, 0.05, 0.1$, and 0.2 for $Ce_{1-x}Sr_xVO_{4-0.5x}$ (b); $x = 0, 0.05, 0.1, 0.2, 0.3$, and 0.4 for $Ce_{1-x}Ca_xVO_{4-0.5x}$ (c); $x = 0, 0.05, 0.1, 0.2, 0.3, 0.4, 0.5$, and 0.625 for $Ce_{1-x}Bi_xVO_4$ (d).

bands is striking for $Ce_{1-x}Ca_xVO_{4-0.5x}$ with $x > 0.2$, which exhibits remarkable lattice contraction and relatively high x_{max} (≈ 0.41). Besides, the 847-cm^{-1} A_{1g} symmetric stretch mode shifts upward, whereas the 372-cm^{-1} $A_{1g} + B_{1g}$ deformation mode and the 261-cm^{-1} mode shift downward with x, as is easily observed for $Ce_{1-x}Ca_xVO_{4-0.5x}$. We also notice that the three broad bands do not manifest themselves in the Raman spectra of $Ce_{1-x}Bi_xVO_4$, in which the characteristic Raman modes simply change in frequency, linewidth, and intensity with x. Thus, there exist some interesting spectroscopic distinctions between the solid solutions of $Ce_{1-x}M_xVO_{4-0.5x}$ and $Ce_{1-x}Bi_xVO_4$ which are formed by substituting aliovalent or isovalent cations with different/similar ionic radii for Ce in $CeVO_4$, respectively.

To determine why the three broad bands appear in $Ce_{1-x}M_xVO_{4-0.5x}$ alone but not in $Ce_{1-x}Bi_xVO_4$, Fig. 3 presents the intensity (arbitrary units) of the 705 cm^{-1} broad band as a function of oxygen stoichiometry, 4–0.5x, for $Ce_{1-x}Ca_xVO_{4-0.5x}$. It should be noted that a change in oxygen stoichiometry is induced to preserve the charge neutrality when aliovalent Ca is substituted for Ce. There exists a good correlation between two parameters, revealing that the intensity increases nonlinearly with the change in oxygen stoichiometry. Consequently, we guess that the change in oxygen stoichiometry is responsible for the appearance of the broad bands at 495, 705, and 912 cm^{-1} in $Ce_{1-x}M_xVO_{4-0.5x}$.

Meanwhile, the charge transfer effect on the aliovalent cation substitution, which preserves the charge neutrality via the change in oxygen stoichiometry (9), could be connected with the remarkable enhancement in electrical conductivity in $Ce_{1-x}Ca_xVO_{4-0.5x}$ over $Ce_{1-x}Bi_xVO_4$ relative to $CeVO_4$ (4). Also, the change in oxygen stoichiometry, i.e., the introduction of oxygen deficiency, caused chemical/structural modifications, for example, by altering the local coordination around the V atoms from the VO_4 to VO_3 tetrahedra. This local coordination change results in shortening of V–O bonds while the V atoms remains in the pentavalent, which could be associated with the appearance of the broad bands. In addition, the chemical/structural modifications would provide the different phonon density of states or disorder-induced Raman modes observed in TiO_2 (17, 18), hence distinctive spectral changes between $Ce_{1-x}M_xVO_{4-0.5x}$ and $Ce_{1-x}Bi_xVO_4$. Further investigation is reported elsewhere.

In Fig. 4, the Raman shift of the 847 cm^{-1} A_{1g} symmetric stretch mode (ν_1) is plotted as a function of x for $Ce_{1-x}M_xVO_{4-0.5x}$ (M = Pb, Sr, and Ca) and $Ce_{1-x}Bi_xVO_4$. The Raman shift of the mode exhibits a considerable increase with x for $Ce_{1-x}Ca_xVO_{4-0.5x}$ and

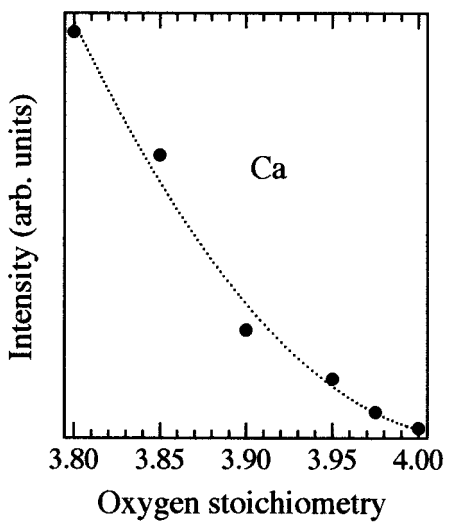

FIG. 3. The intensity (arbitrary units) of the broad Raman band at 705 cm^{-1} as a function of oxygen stoichiometry, $4 - 0.5x$, for $Ce_{1-x}Ca_xVO_{4-0.5x}$.

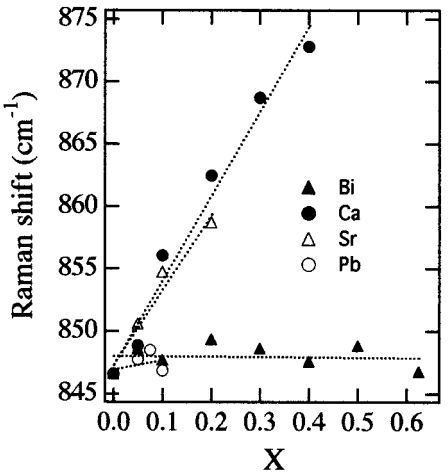

FIG. 4. The Raman shift of the A_{1g} symmetric stretch mode (v_1) at 847 cm^{-1} as a function of x for $Ce_{1-x}M_xVO_{4-0.5x}$ (M = Pb, Sr, and Ca) and $Ce_{1-x}Bi_xVO_4$.

$Ce_{1-x}Sr_xVO_{4-0.5x}$, whereas it is marginal with x for $Ce_{1-x}Pb_xVO_{4-0.5x}$ and $Ce_{1-x}Bi_xVO_4$. The x-dependent Raman shift of the A_{1g} symmetric stretch mode can be reconciled with the lattice contraction as shown in Fig. 1. The lattice contraction unequivocally shortens the V–O lengths; hence the A_{1g} symmetric stretch mode (v_1), which corresponds to the stretching vibration of the VO_4 group, should harden accordingly. As a matter of fact, the V–O lengths systematically shorten with decreasing lanthanide ionic radius in lanthanide vanadates $LnVO_4$ (2), which reduces the lattice parameters a and c, giving rise to the lattice contraction. For $Ce_{1-x}M_xVO_{4-0.5x}$ and $Ce_{1-x}Bi_xVO_4$, the cell volume decreases with x; thus, we expect that the V–O lengths shorten and the Raman shift increases with x. However, it is of interest that $Ce_{1-x}Sr_xVO_{4-0.5x}$ and $Ce_{1-x}Bi_xVO_4$ exhibit almost the same lattice contraction up to $x = 0.3$, but they reveal quite different x-dependent Raman shifts of the A_{1g} symmetric stretch mode.

Namely, the former shows an x-dependent Raman shift similar to that of $Ce_{1-x}Ca_xVO_{4-0.5x}$, whereas there is no noticeable increase in the Raman shift with x for $Ce_{1-x}Bi_xVO_4$. This implies that the relation as shown in Fig. 4, which depends on the kind of substitutions, cannot be explained in terms of lattice contraction alone. It is probable that the distortion of VO_4 tetrahedra is regarded as another relevant factor, as expected for the 372-cm^{-1} mode. Furthermore, we are not able to overlook a mass effect on the Raman modes' frequency. Note that the mass difference between the cations X, which are replaced by other cations, exerts a strong influence on the Raman modes' frequency in the molybdate and tungstate solid solutions $XMoO_4$ or XWO_4 with X being Sr, Ba, Pb, and Ca (19). Analogously, different mass ratios (for example, Bi/Ce = 1.43 and Ca/Ce = 0.48) are likely responsible for the x-dependent Raman shift of the 847-cm^{-1} A_{1g} symmetric stretch mode as shown in Fig. 4.

The $A_{1g} + B_{1g}$ deformation mode (v_2) at 372 cm^{-1} softens with x, as shown in Fig. 5. The frequency decrease in the mode can be ascribed to the distortion of VO_4 tetrahedra, which causes a decrease in force constants. As expected, the frequency change of the $A_{1g} + B_{1g}$ deformation mode with x well represents the x-dependent lattice contraction. The substitution of Bi, which induces less lattice contraction, shows a relatively moderate change in frequency with x (linear). However, the substitution of Ca, which induces the pronounced lattice contraction, exhibits a significant decay in frequency with x (nonlinear). For the substitution of Pb, there is the remarkable frequency change of the $A_{1g} + B_{1g}$ deformation mode with x, indicating a large distortion of VO_4 tetrahedra and great difficulty to form $Ce_{1-x}Pb_xVO_{4-0.5x}$. The Raman mode at 261 cm^{-1} also decreased in frequency with x (linearly) for $Ce_{1-x}M_xVO_{4-0.5x}$ (M = Pb, Sr, and Ca) and $Ce_{1-x}Bi_xVO_4$, but with no dependence on the kinds of substitutes.

Infrared Spectra

Figure 6 exhibits the infrared absorption spectra of $Ce_{1-x}M_xVO_{4-0.5x}$ (M = Pb, Sr, and Ca) and $Ce_{1-x}Bi_xVO_4$ as a function of x between 400 and 1250 cm^{-1}. The infrared spectrum of $CeVO_4$ is compared with previously reported spectra (14, 17), while more features are detected in the present spectra. Three infrared modes are observed at 450, 750, and 850 cm^{-1}, which are

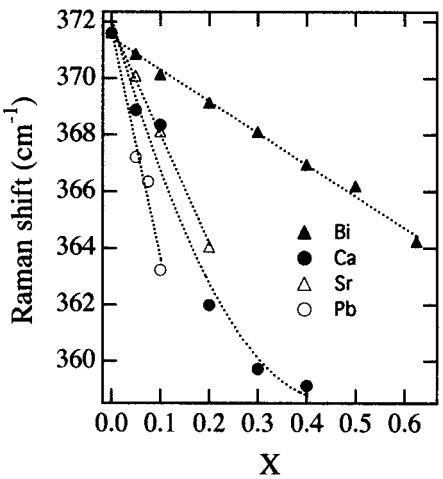

FIG. 5. The Raman shift of the $A_{1g} + B_{1g}$ deformation mode (v_2) at 372 cm^{-1} as a function of x for $Ce_{1-x}M_xVO_{4-0.5x}$ (M = Pb, Sr, and Ca) and $Ce_{1-x}Bi_xVO_4$.

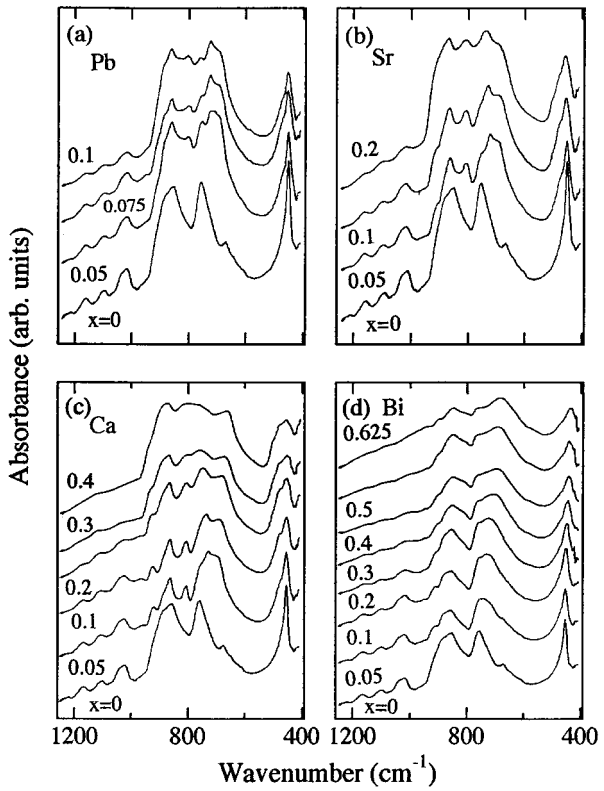

FIG. 6. The infrared absorption spectra of $Ce_{1-x}M_xVO_{4-0.5x}$ (M = Pb, Sr, and Ca) and $Ce_{1-x}Bi_xVO_4$ as a function of x in the wavenumber region 400–1250 cm^{-1}. x = 0, 0.05, 0.075, and 0.1 (from bottom to top) for $Ce_{1-x}Pb_xVO_{4-0.5x}$ (a); x = 0, 0.05, 0.1, and 0.2 for $Ce_{1-x}Sr_xVO_{4-0.5x}$ (b); x = 0, 0.05, 0.1, 0.2, 0.3, and 0.4 for $Ce_{1-x}Ca_xVO_{4-0.5x}$ (c); x = 0, 0.05, 0.1, 0.2, 0.3, 0.4, 0.5, and 0.625 for $Ce_{1-x}Bi_xVO_4$ (d).

assigned as $E_u + A_{2u}$ deformation (v_4), E_u asymmetric stretch (v_3), and A_{2u} asymmetric stretch (v_3), respectively (2, 15, 16). The E_u and A_{2u} asymmetric stretch modes are somewhat separated, exhibiting multiphonon modes above 950 cm^{-1} (14). We can see that both the E_u and the A_{2u} asymmetric stretch modes undergo noticeable changes in frequency, linewidth, and intensity with x.

As for $Ce_{1-x}Bi_xVO_4$, for example, the 750-cm^{-1} E_u asymmetric stretch mode decreases in strength as another mode tends to emerge at lower wavenumber sides and grow with x. For $Ce_{1-x}M_xVO_{4-0.5x}$ (M = Pb, Sr, and Ca), on the other hand, an additional infrared mode(s) appears between the E_u and A_{2u} asymmetric stretch modes, exhibiting more complex spectra. The spectral changes in the wavenumber region 700–900 cm^{-1} are associated with changes in the V–O bonds in VO_4 tetrahedra (20). However, no quantitative analysis is possible because of the complicated spectra.

Here we focus on the $E_u + A_{2u}$ deformation mode (v_4) at 450 cm^{-1}, which could change in characteristics with x for $Ce_{1-x}M_xVO_{4-0.5x}$ as well as for $Ce_{1-x}Bi_xVO_4$. Because no remarkable frequency change was detected, FWHM (full width at half maximum) of the mode or linewidth is plotted as a function of x for $Ce_{1-x}M_xVO_{4-0.5x}$ (M = Pb, Sr, and Ca) and $Ce_{1-x}Bi_xVO_4$ in Fig. 7. The $E_u + A_{2u}$ deformation mode exhibits almost the same trend of increase in FWHM with x (nonlinear) for $Ce_{1-x}M_xVO_{4-0.5x}$ (M = Pb, Sr, and Ca). However, the mode shows a smaller increase in FWHM with x (linear) for $Ce_{1-x}Bi_xVO_4$. The large increase in FWHM with x for $Ce_{1-x}M_xVO_{4-0.5x}$ can be ascribed to the appearance of the new band around 490 cm^{-1}, which is absent in $Ce_{1-x}Bi_xVO_4$, as is obvious in the Raman spectra of $Ce_{1-x}M_xVO_{4-0.5x}$ (see Fig. 2). Because the 450 cm^{-1} mode cannot be resolved adequately, a large/nonlinear increase in FWHM with x is expected as a result of overlapping modes for $Ce_{1-x}M_xVO_{4-0.5x}$, whereas a small/linear increase in FWHM is predominant for $Ce_{1-x}Bi_xVO_4$ with no new band.

CONCLUSION

The Raman and infrared spectra of $Ce_{1-x}M_xVO_{4-0.5x}$ (M = Pb, Sr, and Ca) and $Ce_{1-x}Bi_xVO_4$ were recorded as a function of x, for a spectroscopic study of substitutional solid solutions. When aliovalent or isovalent cations with similar/different ionic radii were substituted for Ce in $CeVO_4$, it was found that the valence and/or ionic radii of the substitutes dominated the solid solubility limit, producing different lattice parameter changes/distinctive spectral features with x between $Ce_{1-x}M_xVO_{4-0.5x}$ and $Ce_{1-x}Bi_xVO_4$. The broad Raman bands emerge and gain intensity with x in $Ce_{1-x}M_xVO_{4-0.5x}$, while they are absent in $Ce_{1-x}Bi_xVO_4$, which could be associated with a change in oxygen stoichiometry to preserve the charge

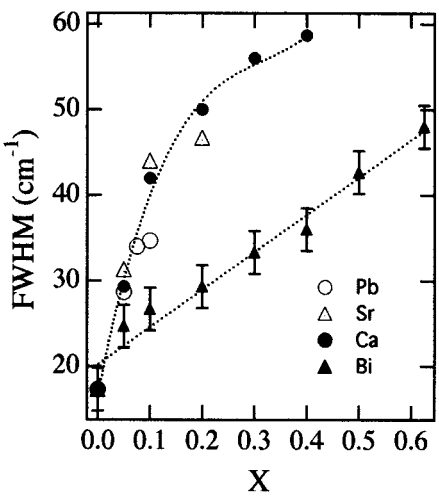

FIG. 7. Variation in FWHM of the $E_u + A_{2u}$ deformation mode at 450 cm^{-1} with x for $Ce_{1-x}M_xVO_{4-0.5x}$ (M = Pb, Sr, and Ca) and $Ce_{1-x}Bi_xVO_4$; the dotted lines are only a visual guide.

neutrality when aliovalent cations are substituted for Ce. The x-dependence of frequency, linewidth, and intensity of the Raman/infrared modes is presented and discussed to draw a spectroscopic distinction between $Ce_{1-x}M_xVO_{4-0.5x}$ and $Ce_{1-x}Bi_xVO_4$ solid solutions.

ACKNOWLEDGMENTS

We are grateful to F. Fujishima of MST (Foundation for Promotion of Materials Science and Technology of Japan) for the Raman scattering measurements. This work was supported by CREST of Japan Science and Technology.

REFERENCES

1. H. Fuess and A. Kallel, *J. Solid State Chem.* **5,** 11 (1972).
2. B. C. Chakoumakous, M. M. Abraham, and L. A. Boather, *J. Solid State Chem.* **109,** 197 (1994).
3. M. Yoshimura and T. Sata, *Bull. Chem. Soc. Jpn.* **42,** 3195 (1969).
4. A. Watanabe, *J. Solid State Chem.* **153,** 174 (2000).
5. K. Gaur and H. B. Lal, *J. Mater. Sci.* **20,** 3167 (1985).
6. R. F. Reidy and K. E. Swider, *J. Am. Ceram. Soc.* **78,** 1121 (1995).
7. R. Beyers and T. M. Shaw, *in* "Solid State Physics," Vol. 42, p. 135. Academic Press, San Diego, 1989.
8. X. H. Chen, K. Q. Ruan, G. G. Qian, S. Y. Li, L. Z. Cao, J. Zou, and C. Y. Xu, *Phys. Rev. B* **58,** 5868 (1988).
9. M. Kakihana, M. Osada, M. Käll, L. Börjesson, H. Mazaki, H. Yasuoka, M. Yashima, and M. Yoshimura, *Phys. Rev. B* **53,** 11796 (1996).
10. D. Palles, N. Poulakis, E. Liarokapis, K. Conder, E. Kaldas, and K. A. Müller, *Phys. Rev. B* **54,** 6721 (1996).
11. T. Hirata, K. Ishioka, M. Kitajima, and H. Doi, *Phys. Rev. B* **53,** 8442 (1996).
12. T. Hirata, M. Kitajima, K. G. Nakamura, and E. Asari, *J. Phys. Chem. Solids* **55,** 349 (1994).
13. R. D. Shannon, *Acta Crystallogr. A* **32,** 751 (1976).
14. U. Opara Krasovec, B. Orel, A. Surca, N. Bukovec, and R. Reisfeld, *Solid State Ionics* **118,** 195 (1999).
15. E. J. Baran and P. J. Aymonino, *Z. Anorg. Allg. Chem.* **383,** 226 (1971).
16. E. J. Baran, M. E. Escobar, L. L. Fournier, and R. R. Filqueira, *Z. Anorg. Allg. Chem.* **472,** 193 (1981).
17. N. Suresh Rao and O. G. Palanna, *Bull. Mater. Sci.* **18,** 593 (1995).
18. M. Ocana, V. Fornes, J. V. Grarcia-Ramos, and C. J. Serna, *J. Solid State Chem.* **75,** 364 (1998).
19. M. Liegeois-Duyckaerts and P. Tarte, *Spectrochim. Acta* **28A,** 2037 (1972).
20. S. P. S. Porto, P. A. Fleury, and T. C. Damen, *Phys. Rev.* **154,** 522 (1967).